scientific reports

Check for updates

OPEN

Tailoring the mechanical strength and corrosion resistance of aluminum matrix composites through biochar reinforcement at varied weight percentages

Ibrahim A. Alnaser

This study introduces an innovative approach to fabricate aluminum matrix composites strengthened with biochar, derived from renewable biomass sources. A systematic investigation of varying biochar weight percentages (0, 2.5, 5, 7.5, and 10 wt%) reveals substantial improvements in mechanical properties and corrosion resistance. Mechanical assessments, including compressive strength and hardness, demonstrate a significant enhancement in mechanical strength with biochar incorporation. In this study, it was discovered that the composite with 7.5 wt% biochar exhibits an optimal balance, displaying an 8.83% increase in compressive strength and a 15.15% rise in hardness compared to the base aluminum matrix. The study further evaluates corrosion behavior through electrochemical analyses and immersion tests in 3.5% NaCl corrosive environments, highlighting the superior corrosion resistance of biochar-reinforced composites. Corrosion rates decrease by 73% in the composite with 10 wt% biochar for the 24 h immersion time, affirming its protective barrier against corrosive agents. This research provides quantitative insights into tailoring mechanical and corrosion properties in aluminum matrix composites through biochar reinforcement, offering a promising avenue for sustainable material development. The resulting materials exhibit not only an 8.83% increase in mechanical strength but also a 73% reduction in corrosion rates, offering valuable uses in industries that need strong, eco-friendly solutions.

Keywords Eco-friendly alloys, Aluminum matrix composites, Biochar reinforcement, Mechanical properties, Corrosion resistance

In the dynamic landscape of materials science, the continual pursuit of advanced materials exhibiting exceptional mechanical properties and heightened resistance to corrosion is a cornerstone of innovation. This important motivation is highlighted by the ever-growing range of applications in aerospace[1,2], automotive[3], and structural engineering[4], where materials must meet high standards of performance and durability[5]. Against this backdrop, the integration of sustainable additives has emerged as an essential area of exploration, reflecting a global commitment to environmentally aware engineering solutions. This manuscript begins a thorough investigation, diving into the detailed field of aluminum matrix composites strengthened with biochar—a sustainable additive derived from renewable biomass[6–8].

The synthesis of novel materials has been a recurrent theme in materials science, seeking to surpass the limitations of conventional materials and unlock unprecedented possibilities. Biochar, arising from the pyrolysis of organic matter, has garnered attention for its unique structural composition, rich carbon content, and multifaceted applications[9,10]. Beyond its established roles in soil amendment and carbon capture, biochar has increasingly become a focal point in materials research, with potential implications for enhancing the mechanical properties of composites[11–13].

The intersection of biochar with metal matrix composites (MMCs) signifies a promising frontier in materials engineering. The potential to leverage the benefits of aluminum—a material famous for its lightweight design and corrosion resistance—combined with the reinforcing attributes of biochar, presents an innovative path for

Mechanical Engineering Department, College of Engineering, King Saud University, 11421 Riyadh, Saudi Arabia. email: ianaser@ksu.edu.sa

developing sustainable materials. While biochar has demonstrated its effectiveness as a reinforcing agent in various matrices, its incorporation into aluminum matrix composites AMC remains a relatively unexplored domain[14–16].

The motivation for this study arises from a dual objective: the tailoring of mechanical strength and corrosion resistance in aluminum matrix composites. This endeavor is based on the understanding that conventional reinforcement materials, such as ceramic particles or carbon nanotubes, have been extensively investigated. However, the integration of biochar introduces a subtle variable, revealing not only the inherent properties of aluminum but also the unique characteristics specific to biochar.

The research is deeply rooted in a sustainable engineering approach, emphasizing the intentional selection of biochar as a reinforcement material. This choice is in line with the broader global trend towards sustainability. Past studies have demonstrated the effectiveness of biochar in improving mechanical properties and thermal stability in polymers[17] and ceramics[18]. This manuscript aims to expand on these findings, delving into the collaborative effects between aluminum and biochar. The goal is to contribute to the development of sustainable solutions in materials engineering.

Abdo et al. innovatively introduced biochar as a sustainable LDPE reinforcement, achieving uniform blending via a twin-screw extruder and successful composite production through injection molding[17]. The study revealed that biochar significantly enhanced thermal stability, reduced melt flow index, improved hardness (24.3% increase with 10 wt% biochar), and optimized tensile performance. Most remarkably, biochar emerged as an effective solid lubricant, showcasing remarkable wear resistance and reduced friction coefficients—56.3% lower than pure LDPE in the LDPE10 composite.

Udaya and Peter Fernandes have successfully synthesized carbon nanotube-fly-ash (CNT-FA) reinforced aluminum composites, exhibiting enhanced hardness and low wear rates[19]. While Sabitha Jannet et al. successfully employed the stir casting technique to embed Neem Seed Biochar Extract ash particles in aluminum 6061, resulting in different weight percentages of MMCs. The incorporation of 7.5 wt% biochar demonstrated improved tensile strength by approximately 18% and exhibited the least wear rate, showcasing the potential for eco-friendly Advanced Metal Matrix Composites (AMMCs) with enhanced mechanical properties[20].

The systematic exploration of varying weight percentages of biochar (ranging from 0 to 10 wt%) in aluminum matrix composites forms the core of this study. This approach is supported by the intent to unravel the relationship between the concentration of biochar and the resulting equilibrium between mechanical toughness and corrosion prevention. The thorough examination of these composites spans an array of mechanical tests, including tensile strength, hardness, and impact resistance, alongside a comprehensive analysis of their corrosion behavior in diverse environmental conditions.

Materials and methods

In this study, we focused on the base metal matrix, Aluminum fine powder, which was obtained from Merck, Darmstadt, Germany. This powder featured an impressive purity level of 99% and had a particle size diameter ranging between 100 to 200 µm. As for the additives or reinforcement used in our experiment, we utilized biochar that was produced in our own laboratory. The biochar was derived from agricultural waste, allowing us to effectively repurpose and transform this waste material into a valuable resource for our study.

Different techniques are employed to achieve a homogeneous dispersion of biochar within the aluminum matrix in order to prepare the Al/Biochar composite samples. In this current study, the high-energy ball-milling process is utilized to effectively blend the aluminum powder with biochar, ensuring a uniform distribution of the biochar particles throughout the matrix. To begin, the aluminum powder was subjected to a 30-min treatment in a stainless-steel jar and a planetary ball mill. This step was critical in breaking down any agglomerated powder particles and promoting better dispersion. The Desktop 220 V High Energy Vibratory Ball Mill is specifically used with an 80 mL jar from Across International Company, based in Livingston, MT, USA. Next, the biochar was added to the aluminum powder at different weight fractions (0, 2.5, 5, 7.5, and 10 wt.%) and mixed for half an hour. This step ensured the even distribution of biochar within the aluminum matrix, creating a homogenous blend.

Upon preparation of the Al/Biochar mixture, the consolidation process took place in a High-Frequency Induction Heat Sintering (HFIHS) furnace, employing the HF Active Sinter System manufactured by ELTek CO. in Gyeonggi-do, Republic of Korea. The Al/Biochar powder blend was loaded into a graphite die with dimensions of 10 mm inner diameter and 15 mm height. The sintering temperature was precisely controlled using an optical pyrometer from Thermalert TX, supplied by Raytek GmbH in Berlin, Germany. Throughout the sintering process, the mixture underwent a pressure of 40 MPA and was heated at a rate of 100 °C/min until reaching a temperature of 580 °C. To avoid oxidation of the composite samples, the sintering occurred within a vacuum chamber maintaining a pressure of 1×10^{-3} Torr. Subsequent to the completion of the sintering process, the Al/Biochar samples underwent a controlled cooling phase until room temperature was achieved. This cooling step proved critical to ensure the stability and integrity of the composite samples, laying the foundation for subsequent analyses and testing.

The morphology of the produced Al/Biochar composite samples was carefully analyzed using a field emission scanning electron microscope (JEOL; JSM7600F) after conducting corrosion tests. This analysis allowed us to examine the physical characteristics and structural integrity of the composites at a microscopic level. To further investigate the physical properties of the Al/Biochar composite, we evaluated the density of each composition using Archimedes' principle. This measurement provided valuable insights into the mass and volume relationship of the composites, in which we can judge the successfully of the sintering process.

In order to assess the mechanical properties of the produced composites, hardness and compression properties were measured. To determine the hardness, each sample was polished and subjected to a Vickers hardness

test using a ZHVμ-S Micro Vickers Hardness Tester from Zwick/Roell, Ulm, Germany. The test was conducted with a load of 200 g and a dwell time of 10 s. To ensure accurate results, the average hardness was calculated from five samples of each composite, and the standard error was also determined. Additionally, compression tests were performed on the Al/Biochar composite samples in accordance with the ASTM E9-89a standard[21]. These tests were conducted using an INSTRON testing machine with a load capacity of 150 kN (model 3385H). The crosshead was moved at a speed of 2 mm/min during the tests, and each composition was tested using five samples. This allowed us to assess the compressive strength and behavior of the composites under applied loads.

Electrochemical experiments and corrosion studies were conducted on the produced Al/Biochar composite samples using a Potentiostat Autolab (PGSTAT302N) from Metrohm, based in Amsterdam, The Netherlands. The test medium used for these experiments was a 3.5% NaCl solution, which is commonly employed to simulate corrosive environments. For the electrochemical cell setup, a standard three-electrode configuration was utilized. The cell had a capacity of 30 mL and contained the 3.5% NaCl solution. The Al/Biochar composite samples served as the working electrode, while an Ag/AgCl electrode was used as the reference electrode. A Platinum strip (Pt) was employed as the auxiliary or counter electrode. This setup allowed for accurate measurements and control of the electrochemical reactions occurring at the surface of the composite samples.

To obtain Electrochemical Impedance Spectroscopy (EIS) data, the measurements were performed at the open-circuit potential value. A sinusoidal wave perturbation with an amplitude of – 5 mV was applied at the corrosion potential (ECorr). The frequency range for the EIS measurements spanned from 100 MHz to 100 mHz. This technique provided valuable information about the electrical properties and corrosion behavior of the Al/Biochar composites. Cyclic Potentiodynamic Polarization (CPP) experiments were also conducted to assess the corrosion resistance of the composite samples. The potential was scanned between – 1600 mV and + 100 mV (Ag/AgCl) at a scanning rate of 1.5 mV/s. This allowed for the determination of the corrosion potential and the evaluation of the corrosion kinetics and behavior of the composites under varying potentials.

To ensure accurate and reliable results, the tested surface area of all samples was kept constant at $\pi/4$ $(10\ mm)^2 \cong 78.5\ mm^2$. Prior to each test, the samples were cleaned with acetone, washed with distilled water, and dried with air. They were then polished using emery paper and cloth-polished with alumina slurry. To ensure the repeatability of the results, each test was performed at least three times. This rigorous approach helped to minimize experimental variations and ensure the reliability of the obtained data. By conducting these electrochemical experiments and corrosion studies, we aimed to gain insights into the corrosion resistance and behavior of the produced Al/Biochar composite samples in a 3.5% NaCl solution, providing valuable information for potential applications in corrosive environments.

Results and discussion

Reinforcement characterization

The Scanning Electron Microscopy (SEM) micrographs of the biochar, which was produced for the purpose of reinforcing the aluminum matrix, are presented in Fig. 1. These images, captured at varying magnifications, reveal a high degree of porosity in the particulate biochar. The average particle size of the biochar was found to be between 30 and 90 μm, while the average pore size ranged from 3 to 15 μm. This porous structure is beneficial for enhancing the mechanical properties and providing a larger surface area for potential applications.

To investigate the chemical composition of the biochar, Energy-Dispersive X-ray Spectroscopy (EDS) was employed. The results obtained from the EDS analysis indicate that the biochar is primarily composed of carbon and oxygen. Additionally, minor residual elements of sodium, calcium and potassium were detected. It is important to note that the presence of platinum in the EDS pattern is attributed to the platinum coating applied to the sample prior to imaging. This coating serves to enhance the conductivity of the sample's surface, thereby reducing the charging effect during SEM imaging. The percentage of Platinum was excluded from the elemental results to avoid its effect on the results, and that is why the peak of Pt is free of its label in the EDS pattern. The SEM micrographs and EDS analysis provide valuable insights into the morphology and chemical composition of the biochar used as reinforcement in the Al/Biochar composite. The porous structure and elemental composition of the biochar contribute to its potential as a reinforcing material in the composite matrix, offering opportunities for improved mechanical and functional properties.

Mechanical behavior evaluation

Density measurements

The rule of mixture is a concept used in MMC, such as Al + biochar, to predict the overall properties based on individual components. In the case of high-frequency sintering, the relative density of the samples plays a critical role in assessing quality. Achieving a high relative density indicates effective densification and consolidation during sintering, leading to improved mechanical properties. The relative density of each composite is presented in Table 1 and Fig. 2.

The mixture rule equation for estimating the overall theoretical density of an Al + biochar composite based on the weight fractions and densities of its constituent materials can be expressed as follows:

$$r_c = W_{Al} \times r_{Al} + W_b \times r_b$$

where: ρ_c is the theoretical density of the composite material, W_{Al} and W_b represent the weight fractions of aluminum and biochar respectively, ρ_{Al} and ρ_b denote the densities of aluminum and biochar respectively, 2.7 g/cc and 1.7 g/cc.

The observed trend in relative density across the fabricated Al-biochar composites (AB0, AB2.5, AB5, AB7.5, AB10) can be clarified by considering the introduction of biochar into the aluminum matrix. The relative density systematically decreases as the biochar content increases beyond 5 wt.%. This phenomenon may be attributed to

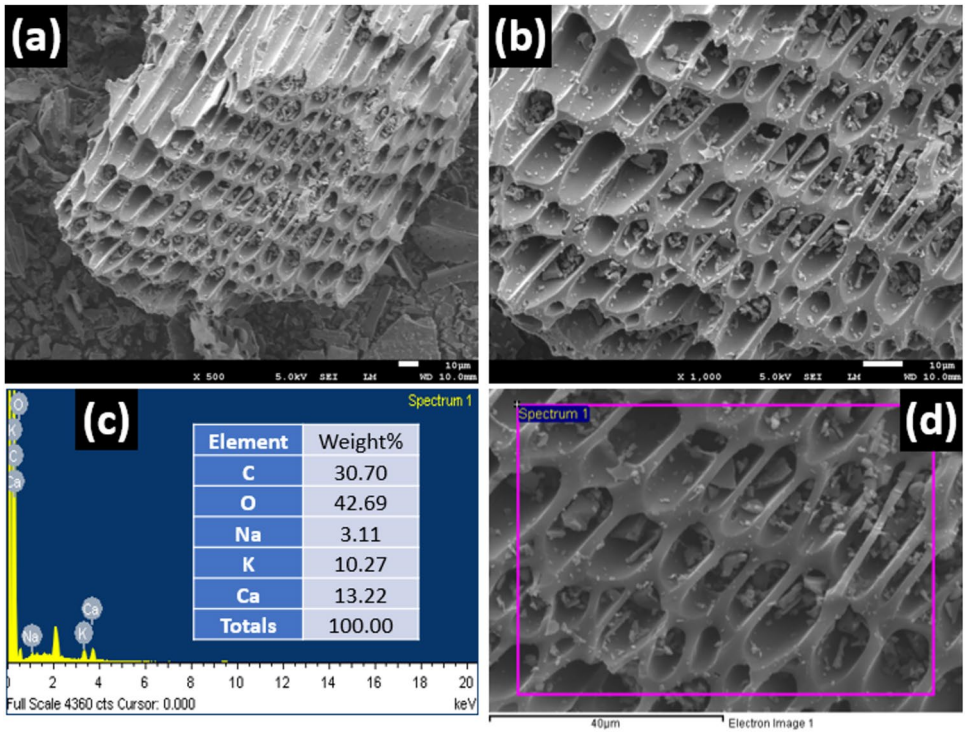

Fig. 1. SEM micrographs for the produced biochar filler at different magnifications (**a**,**b**), (**c**) EDS analysis showing the chemical composition of the biochar, and (**d**) The location where the EDS were taken (area scan).

Sample	Composition	Theoretical density (g/cc)	Measured density (g/cc)	Relative density (%)
AB0	Al pure	2.7	2.7	100.0
AB2.5	Al + 2.5 wt% Biochar	2.64	2.64	100.0
AB5	Al + 5 wt% Biochar	2.61	2.61	100.0
AB7.5	Al + 7.5 wt% Biochar	2.58	2.57	99.6
AB10	Al + 10 wt% Biochar	2.55	2.53	99.2

Table 1. Measurement of density of the Al/Biochar composite samples with different volume fraction of the biochar reinforcement.

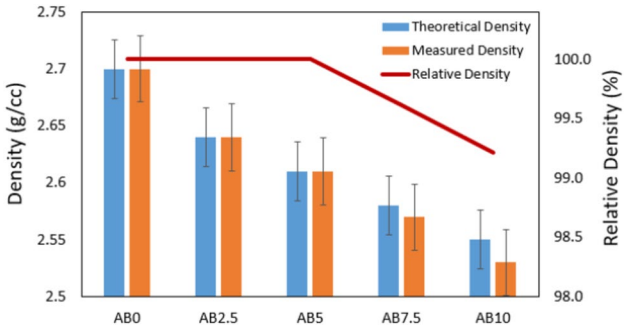

Fig. 2. Theoretical, measured, and relative densities of the Al/Biochar composite samples with different volume fraction of the biochar reinforcement.

the lower density of biochar compared to aluminum. Biochar, derived from biomass pyrolysis, often possesses a lower density due to its porous and lightweight nature. As the weight percentage of biochar increases, the overall density of the composite decreases, impacting the relative density measurements. The porous structure of biochar may introduce voids or spaces within the composite, contributing to the observed reduction in relative density. This trend underscores the importance of considering the density of individual components when formulating metal matrix composites, as varying densities can influence the overall density of the composite material. Furthermore, specific processing methods, such as blending and compaction, can influence the uniform distribution of biochar within the matrix, influencing the final relative density measurements.

Hardness test

Figure 3 represents the variation in Vickers Micro-hardness values across different fabricated composites, utilizing the automated micro-hardness tester. Upon increasing the biochar filler, there is a slight enhancement in the hardness values. It is noteworthy, however, that the change in hardness values for the composite with a higher amount (14.5%) is not significantly substantial. This observation aligns with the increases in the percentage of biochar up to 7.5 wt.%, after which the hardness begins to deteriorate with a continuous increase in the filler percentage.

The observed improvement in hardness can be attributed to the prevention of dislocation movement, which occurs as a result of embedding the biochar filler within the Al matrix[20]. This mechanism effectively inhibits the movement of dislocations, leading to an increase in hardness. Moreover, this strengthening mechanism also contributes to the load-bearing capacity of the composite. These enhancements in mechanical properties can be further explored and discussed in the compression section.

The observed trend in hardness values can be correlated with the previous trend in relative density across the Al-biochar composites. Typically, an increase in relative density is associated with a higher packing density and improved interparticle bonding within the composite. In the context of hardness, the inverse relationship between hardness and the observed decrease in relative density is noteworthy. The reduction in relative density, particularly in AB7.5 and AB10, may suggest an increased prevalence of voids or less effective interparticle bonding, potentially influencing the overall hardness. The porous nature of biochar, contributing to lower density, might introduce variations in the distribution and bonding of particles within the composite, thereby affecting its mechanical properties.

Compression test

The results obtained from the compression tests shown in Fig. 4 provide valuable information into the behavior of the metal matrix composite at different biochar weight percentages. It is intriguing to note that while there is a noticeable increase in ultimate compressive strength (UCS) and stress at 0.6 strain with increasing biochar content, the changes in yield strength (YS) are relatively small. Notably, the UCS exhibits a consistent upward trend with increasing biochar content. This improvement suggests that the incorporation of biochar contributes significantly to the composite's ability to withstand compressive loads. The observed enhancement in UCS aligns with the reinforcing properties typically associated with biochar, reflecting its structural integrity and strength. Additionally, the YS shows nuanced variations, initially decreasing and subsequently increasing with higher biochar content. This behavior underscores the complex interplay between biochar and aluminum in influencing the material's resistance to deformation. The stress at fracture further emphasizes the material's strength, with a substantial increase as biochar content rises. This trend indicates that the composite, particularly in AB7.5 and AB10, exhibits enhanced resistance to failure under compression, showcasing the potential of biochar as a reinforcing agent in MMCs.

The trend observed in the ultimate compressive strength (UCS) values reveals a consistent improvement with increasing biochar content. This enhancement can be attributed to the reinforcing effects of biochar, which is known for its inherent strength and structural integrity. The higher UCS values in AB5, AB7.5, and AB10 suggest that the addition of biochar contributes positively to the composite's ability to withstand compressive

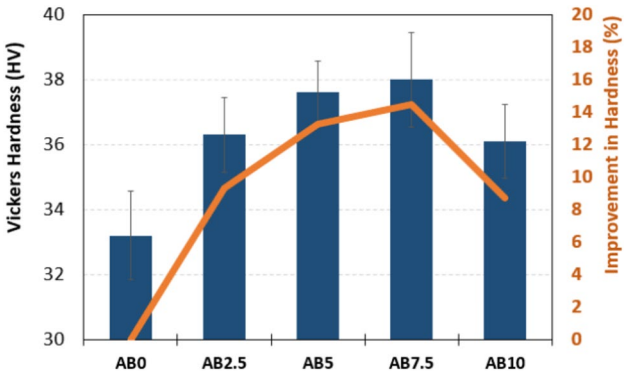

Fig. 3. Vickers hardness values for pure Al and different biochar composite samples.

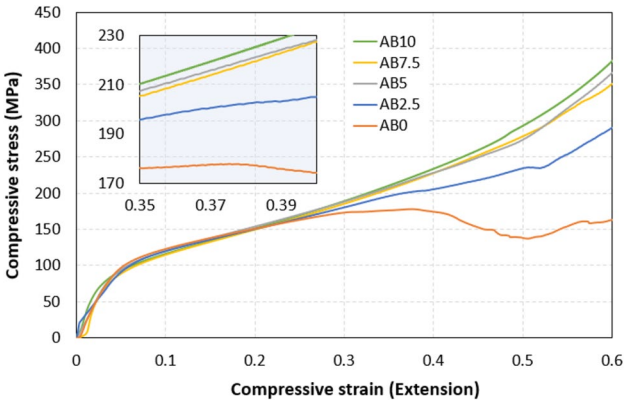

Fig. 4. Compressive stress–strain diagrams for pure Al and different biochar composite samples.

loads. This trend aligns with previous studies where biochar incorporation has demonstrated reinforcing effects in various composite systems[22,23].

Contrary to UCS, the YS trend showing in Fig. 5, exhibits a slight fluctuation with varying biochar content. The initial decrease in YS from AB0 to AB2.5 could be associated with changes in the microstructure or the initiation of yielding at lower stress levels. However, as the biochar content increases beyond 2.5%, there is a subsequent increase in YS, indicating that the biochar reinforcement is influencing the material's ability to resist deformation and undergo plastic flow. Further investigation into the microstructural changes and the mechanisms governing plastic deformation could provide deeper insights into this behavior.

The observed trends in UCS and YS values across the Al-biochar composites can be correlated with the previously discussed hardness and relative density trends. Generally, an increase in hardness is associated with improved material strength, and in this context, the ascending trend in UCS values aligns with the observed increase in hardness, suggesting a positive correlation between the two. This correlation supports the notion that the reinforcing effects of biochar contribute to both hardness and ultimate compressive strength. Conversely, the yield strength trend does not exhibit a consistent relationship with hardness. The stable yield strength values despite variations in hardness and the observed decrease in relative density may suggest that factors beyond hardness and relative density influence the yield behavior of the composites. The complex interplay of biochar content, distribution, and bonding within the aluminum matrix likely contributes to the nuanced mechanical responses observed in UCS and YS.

Corrosion behavior

Potentiodynamic polarization testing

The Potentiodynamic Polarization measurements for the fabricated composite samples immersed in a 3.5% NaCl solution were analyzed in Fig. 6a–c. These curves represent the variations in corrosion behavior after different immersion durations of 1, 24, and 72 h. To provide a comprehensive understanding of the data, Table 2 presents the extracted parameters from the Potentiodynamic Polarization plots. These parameters include the corrosion rate (RCorr), corrosion current density (jCorr), corrosion potential (ECorr), as well as the anodic and cathodic Tafel slopes (βa and βc).

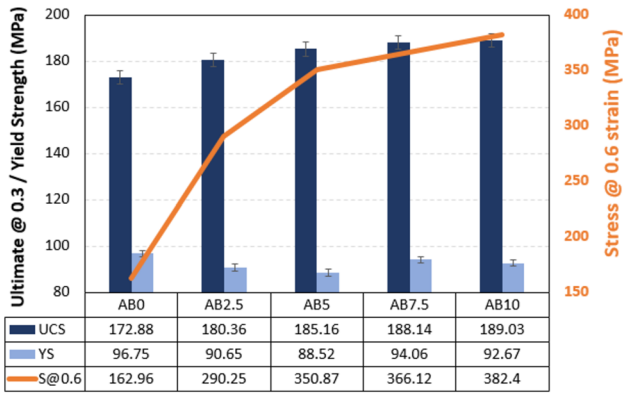

	AB0	AB2.5	AB5	AB7.5	AB10
UCS	172.88	180.36	185.16	188.14	189.03
YS	96.75	90.65	88.52	94.06	92.67
S@0.6	162.96	290.25	350.87	366.12	382.4

Fig. 5. Ultimate compressive stress (UCS), yield strength (YS) and stress at 0.6 strain for pure Al and different biochar composite samples.

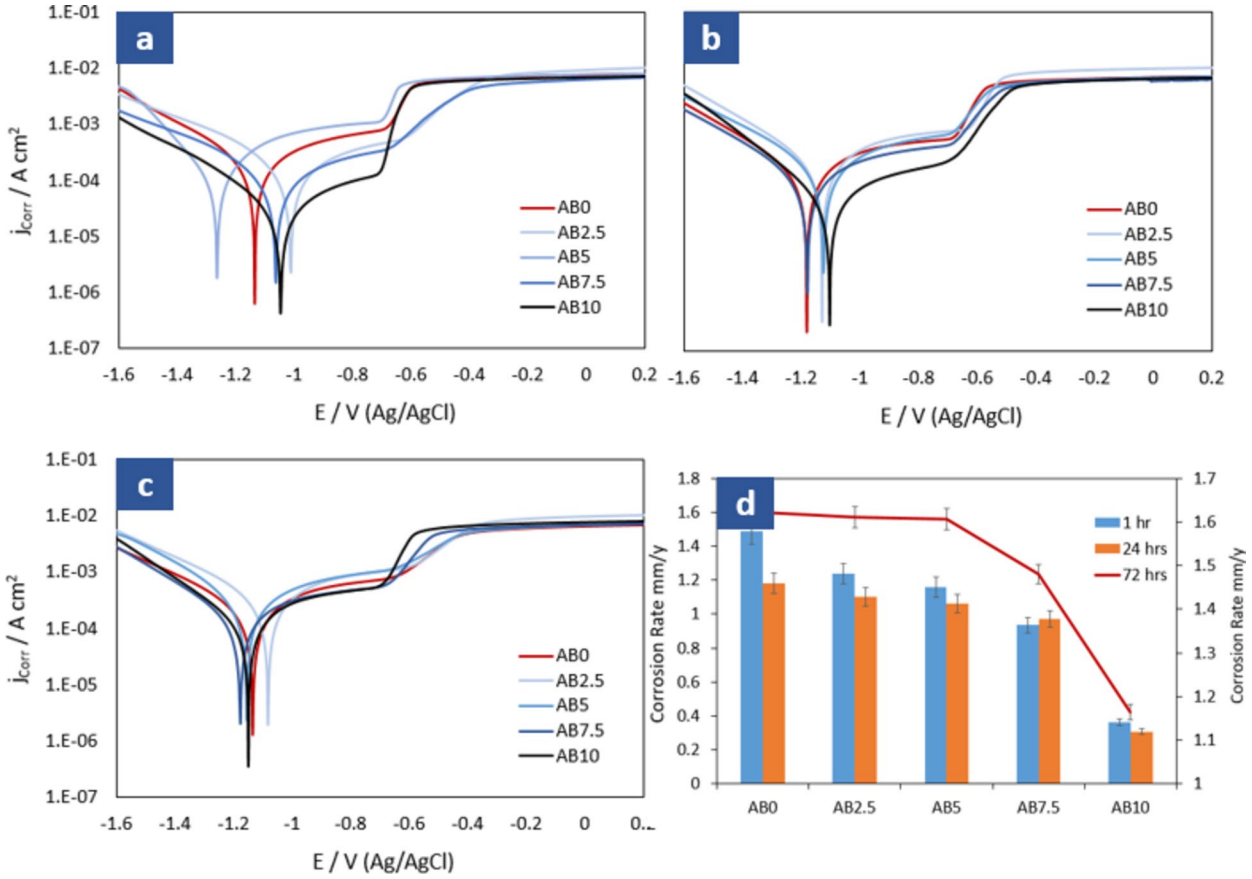

Fig. 6. Potentiodynamic polarization for pure Al and different biochar composite samples exposed in 3.5% NaCl solution for (**a**) 1 h, (**b**) 24 h, (**c**) 72 h, and (**d**) corrosion rate of all samples.

Time	Sample	βc V dec^{-1}	E_{Corr} V	βa V dec^{-1}	j_{Corr} A cm^{-2}	Corrosion rate mm/year
1 h	AB0	0.314	− 1.127	0.262	1.28 E−04	1.485
	AB2.5	0.295	− 1.154	0.213	1.09 E−04	1.238
	AB5	0.251	− 1.274	0.173	9.98 E−05	1.159
	AB7.5	0.43	− 1.05	0.327	8.04 E−05	0.934
	AB10	0.498	− 1.05	0.306	3.11 E−05	0.362
24 h	AB0	0.339	− 1.177	0.284	1.02 E−04	1.179
	AB2.5	0.312	− 1.152	0.256	9.89 E−05	1.102
	AB5	0.265	− 1.122	0.226	9.16 E−05	1.063
	AB7.5	0.266	− 1.182	0.408	8.37 E−05	0.972
	AB10	0.21	− 1.095	0.188	2.66 E−05	0.308
72 h	AB0	0.341	− 1.126	0.321	1.4 E−04	1.621
	AB2.5	0.318	− 1.136	0.265	1.39 E−04	1.611
	AB5	0.281	− 1.158	0.193	1.38 E−04	1.606
	AB7.5	0.503	− 1.179	0.313	1.36 E−04	1.481
	AB10	0.265	− 1.137	0.279	9.16 E−05	1.164

Table 2. Obtained parameters from potentiodynamic polarization plots of the Al/Biochar composite samples with the exposure of 1-h, 24-h and 72-h in 3.5% NaCl solutions with different volume fraction of the biochar reinforcement.

It is important to highlight that the automated calculation of various parameters, encompassing the corrosion rate, was facilitated through the employment of the Autolab software (NOVA 1.8). The determination of icorr (corrosion current) and Ecorr (corrosion potential) from the polarization data was conducted utilizing the Tafel slope method. This extraction procedure involved outlining anodic and cathodic slopes within the NOVA software, subsequently triggering an automatic computation that furnished the accurate values for icorr and Ecorr. This systematic approach not only ensured precision in parameter determination but also streamlined the data analysis process, enhancing the reliability and efficiency of the corrosion assessment.

Analysing the data from Table 2, we can gain insights into the corrosion behavior of the fabricated composite samples immersed in a 3.5% NaCl solution for different durations.

These parameters provide valuable information about the corrosion behavior of the composite samples. The Tafel slopes (βc and βa) indicate the rate of corrosion reactions on the cathodic and anodic sides, respectively. The corrosion potential (ECorr) represents the equilibrium potential at which the anodic and cathodic reactions occur at the same rate. The corrosion current density (jCorr) reflects the rate of electron transfer during the corrosion process. Finally, the corrosion rate quantifies the amount of material lost due to corrosion per year.

By analyzing these parameters, we can observe variations in the corrosion behavior of the composite samples over time. For example, comparing the corrosion rates of AB0–AB10 at the same immersion durations (1-h, 24-h, and 72-h), we can see a noticeable decrease with increasing the biochar percentage. This suggests that the corrosion rate of the fabricated composites is affected positively by the content of the biochar filler. By increasing the reinforcement biochar material in the fabricated nanocomposite sample, there is an observed increase in the passivation of the sample surface[24]. This passivation is evident in the polarization measurements, as the presence of biochar leads to an expansion of the passive region on the curves, accompanied by a reduction in current values. The polarization curves (Fig. 6a–c) further highlights this trend. They demonstrate that the change in corrosion rate between different immersion times (1 h, 24 h, and 72 h) of the samples in 3.5% NaCl solutions is positively decreased by increasing the percentage of reinforcement. This relationship is visually represented in Fig. 6d.

Electrochemical impedance spectroscopy (EIS)

Electrochemical impedance spectroscopy (EIS) is a valuable technique for studying electrochemical systems. In this study, the EIS technique is employed to investigate the electrochemical performance of aluminum composites prepared with varying amounts of biochar. To conduct the electrochemical experiments, an Autolab PGSTAT 30 workstation (Metrohm, Amsterdam, Netherlands) is utilized. A three-electrode cell configuration was employed, with the working electrode being the prepared samples. The counter electrode was a platinum electrode, and the reference electrode used was an Ag/AgCl electrode.

The tests were conducted on the prepared samples after exposing them to a 3.5% NaCl solution. We collected data at different time intervals, specifically after 1 h, 24 h, and 72 h of exposure to the NaCl solution. By performing EIS measurements on these samples, we aimed to gain insights into their electrochemical behavior and performance. EIS allows us to analyze the impedance response of the samples, providing information about their corrosion resistance and the effectiveness of the biochar reinforcement in enhancing their electrochemical properties.

To assess the anticorrosion properties of the prepared aluminum composites with varying amounts of biochar, we employed both EIS and Tafel polarization curves. The EIS was used to obtain the Nyquist spectrum for all the prepared samples after different exposure periods, which is displayed in Fig. 7. This spectrum provides valuable information about the impedance response of the samples and allows us to analyze their corrosion resistance. To fit the EIS spectra, fitting circuits illustrated in Fig. 8 were utilized. The circuits include the following components:

- Rs, which represents solution resistance.
- Rp, which represents polarization resistance or charge transfer resistance.
- CPE, which represents the constant phase element.

Fitting the EIS spectra using this circuit enable the extraction of meaningful results. These results, obtained from the circuit fittings, are presented in Table 3. The obtained results from the circuit fittings provide insights into the electrical behavior and corrosion resistance of the Al/Biochar composites. Analysing parameters such as solution resistance, polarization resistance, and the constant phase element allows for the assessment of the effectiveness of biochar reinforcement in enhancing the anticorrosion properties of the composites.

The obtained Nyquist data reveals interesting insights into the corrosion behavior of the prepared aluminum composites after exposure to 3.5% NaCl solution. After 1-h exposure, a distorted semicircle is observed in the Nyquist plots for all the prepared samples. Initially, the addition of 2.5% biochar filler led to a deterioration in the properties of the composites. However, with the addition of biochar filler starting from 5%, the diameter of the semicircle increased, indicating improved anticorrosive properties. It is widely accepted that a larger semicircle diameter corresponds to higher corrosion resistance[24]. The semicircle diameter enlarges further with increasing percentages of biochar, suggesting enhanced resistance to corrosion. The obtained Nyquist data was fitted with the circuit shown in Fig. 7, and the results of the fitting analysis are presented in Table 3. The addition of biochar material in the aluminum matrix increased the resistance, as evidenced by higher values of polarization resistance (Rp). Higher Rp values indicate the formation of a stable oxide layer on the alloy surface, which acts as a barrier against the penetration of corrosive ions, thereby increasing the corrosion resistance.

The constant phase element (CPE) in the circuit represents a capacitive element that can interpolate between a capacitor and a resistor, depending on the value of "n"[25]. For the prepared alloys, the value of "n" in the CPE falls between 0.6 and 0.85, indicating the presence of double-layer capacitors with some pores on the composite

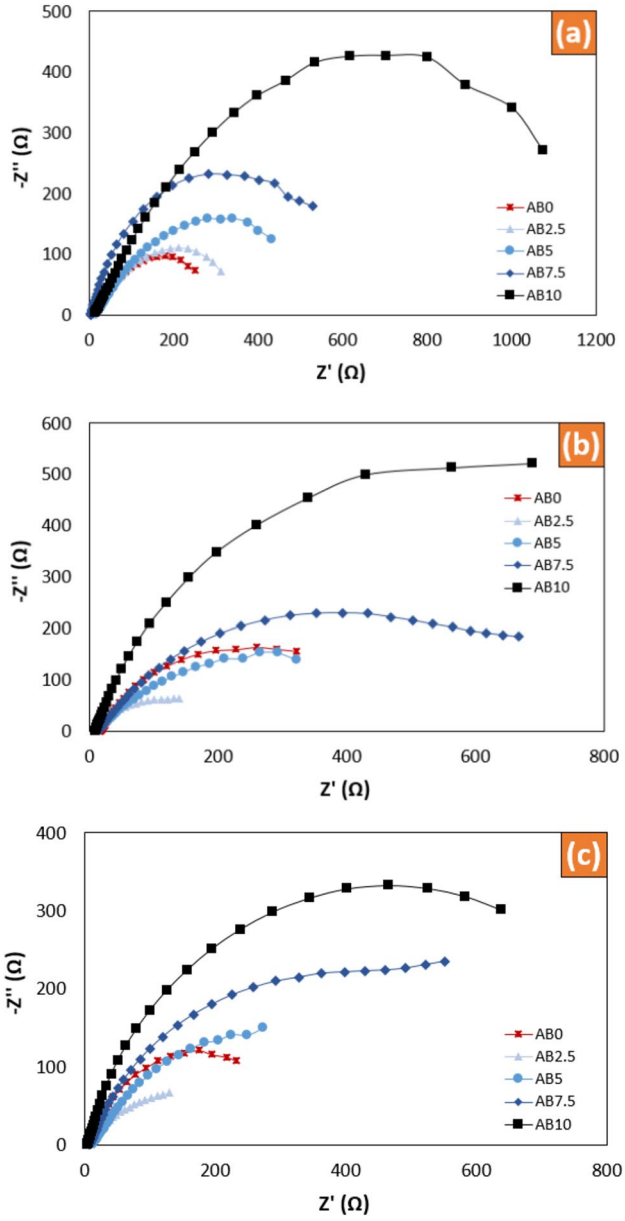

Fig. 7. Obtained Nyquist spectrum for the prepared aluminum composite (**a**) after 1-h exposure (**b**) after 24-h exposure (**c**) after 72-h exposure.

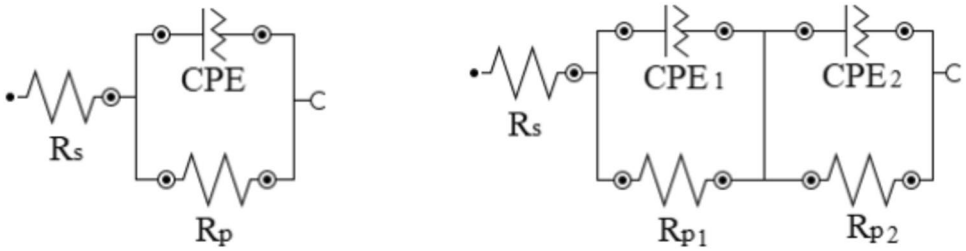

Fig. 8. Circuits used to fit the Nyquist plots.

Time	Sample	Rs	Rp	CPE				
		Ω cm²	Ω cm²	Y0 (mMho)	n			
1 h	AB0	6.11	372	1.31	0.6			
	AB2.5	7.23	438	1.33	0.59			
	AB5	15	698	0.90	0.57			
	AB7.5	3.96	651	0.45	0.80			
	AB10	12.6	1350	0.48	0.85			
24 h	AB0	17.1	480	1.05	0.76			
	AB2.5	8.39	213	2.22	0.68			
	AB5	11.9	619	1.34	0.59			
	AB7.5	13.3	800	0.41	0.67			
	AB10	9.49	1580	0.29	0.65			
72 h	AB0	8.63	335	1.24	0.78			
	AB2.5	9.14	277	2.02	0.63			
	AB5	11.2	604	1.60	0.59			
	AB10	4.22	939	0.37	0.80			
Time	Sample	Rs	Rp_1	Rp_2	CPE1		CPE2	
		Ω cm²	Ω cm²	Ω cm²	Y0 (mMho)	n	Y0 (mMho)	n
72 h	AB7.5	6.89	995	276	1.80	0.563	0.415	0.856

Table 3. Obtained parameters after EIS experiment of the Al/Biochar composite samples with the exposure of 1-h, 24-h and 72-h in 3.5% NaCl solutions with different volume fraction of the biochar reinforcement.

surfaces[26,27]. The passive film formed on the surface of the aluminum alloy is non-uniform and exhibits small porosities[28]. During the testing of the samples, the results indicate that exposure to 3.5% NaCl solution affects the samples, as evidenced by the decrease in the value of CPE with the addition of biochar. These findings suggest that the addition of biochar in the aluminum matrix enhances the corrosion resistance of the composites by promoting the formation of a stable oxide layer and altering the capacitive behavior of the surface. The presence of pores in the passive film could play a role in the electrochemical behavior of the composites.

As the exposure time increased to 24 h, the Nyquist plot showed that the semicircle arc moved to higher values, indicating an improvement in the corrosion resistance properties of the composites. This suggests that a thin oxide layer formed at the surface during contact with water, contributing to the increase in corrosion resistance[29,30]. Additionally, the constant phase element (CPE) decreased, which is believed to be a result of oxide layer formation. The fitting analysis of the data showed that exposure to 24 h enhanced the anticorrosion properties of the prepared material. There was an increase in polarization resistance, indicating the formation of a more stable oxide layer. The CPE values further declined, suggesting the presence of a more uniform and protective oxide layer at the surface.

However, when the exposure time was prolonged to 72 h, the Nyquist plot exhibited a reduction in the semicircle arc to lower values and the appearance of second time constant for sample AB7.5, it emphasis that corrosive species surpassed the oxide barrier reaching metal surface. This indicated a decline in the properties of the samples due to the penetration of water through a porous oxide layer at the surface. The aggressive corrosive ions were able to penetrate the material more deeply, resulting in a reduction in resistance values and an increase in CPE. The prolonged exposure of the samples to water increased the chances of voids exploration as the initially formed oxide layer became stabilized. The fitting of the obtained data revealed that the resistance of the samples decreased after 72 h of exposure, as indicated by the decline in polarization resistance values. However, as confirmed by Bode plots in Fig. 9, the obtained values were still better than those of the original blank samples which aligns with the behavior observed in similar research[31]. These findings suggest that the incorporation of biochar in the composites provided some level of protection against corrosion.

The Scanning Electron Microscope (SEM) images of the corrosion surfaces (Fig. 10) of the five samples provide critical insights into the morphological aspects of the Al/Biochar composites following exposure to the 3.5% NaCl corrosive environments. Examining these images reveals notable features that align with the earlier discussed mechanical and corrosion resistance results. Notably, the composite with 10 wt.% biochar exhibits a corrosion surface with a finer and more uniform corrosion pattern. This observation is indicative of a more controlled corrosion process, potentially enhanced by the protective influence of biochar on the composite surface. Conversely, the sample with 2.5 wt.% biochar, showcasing a deterioration in mechanical properties, displays a corrosion surface with irregular and prominent corrosion features, suggesting a less favourable corrosion resistance. Furthermore, the SEM images validate the positive correlation between increased biochar content and enhanced corrosion resistance, as evidenced by the improved corrosion surfaces in samples with 5 wt.% and higher biochar content. These findings support the quantitative results obtained through electrochemical measurements, where the 10 wt.% biochar-reinforced sample exhibited a remarkable 73.87% improvement in corrosion resistance after 24 h of immersion. The SEM analysis serves as a visual confirmation, linking the structural changes on the corrosion surfaces with the mechanical and electrochemical behaviors of the Al/Biochar

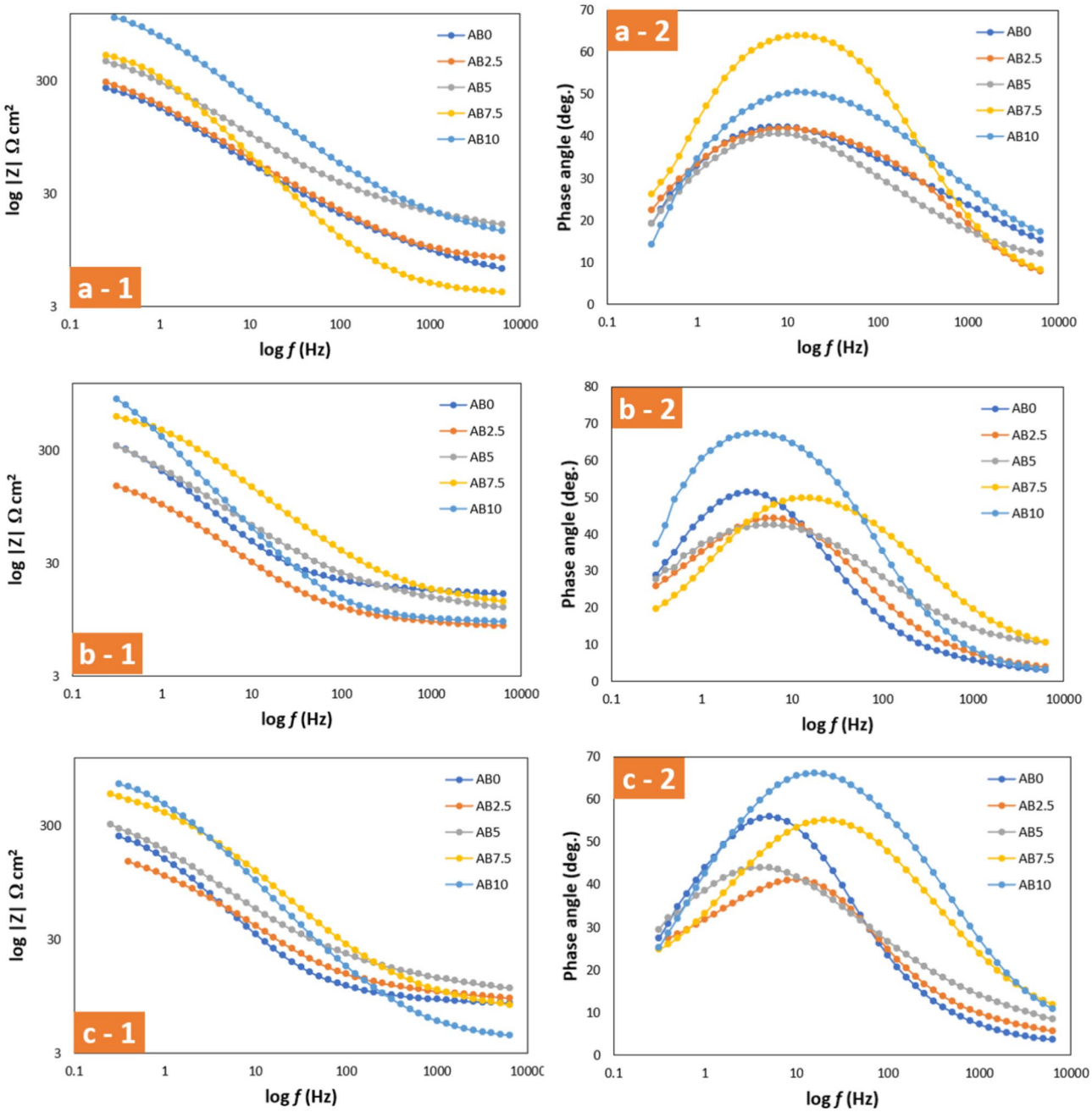

Fig. 9. Bode plots for the prepared aluminum composite (**a**) after 1-h exposure (**b**) after 24-h exposure (**c**) after 72-h exposure, (1) Impedance curves, and (2) Phase angles curves.

composites, thereby providing a comprehensive understanding of the interplay between composition, structure, and performance in these composite materials.

These findings highlight the importance of considering the exposure time when evaluating the corrosion resistance properties of the prepared composites. While the initial exposure time of 24 h improved the anticorrosion properties, prolonged exposure to 72 h led to a deterioration in the performance. Further research is needed to optimize the composition and structure of the composites to enhance their long-term corrosion resistance.

Conclusions

The fabrication of Al/Biochar composites was achieved utilizing a powder metallurgy route. Al powder and biochar were mixed at different compositions using a high-energy ball milling technique. The mixture was then consolidated through inductive sintering at specific conditions. The resulting nanocomposite samples were subjected to characterization, mechanical testing, and electrochemical corrosion testing. The corrosion behavior of the composites was evaluated after immersions of 1 h, 24 h, and 72 h in 3.5% NaCl solutions. Various electrochemical techniques such as electrochemical impedance spectroscopy and cyclic potentiodynamic polarization

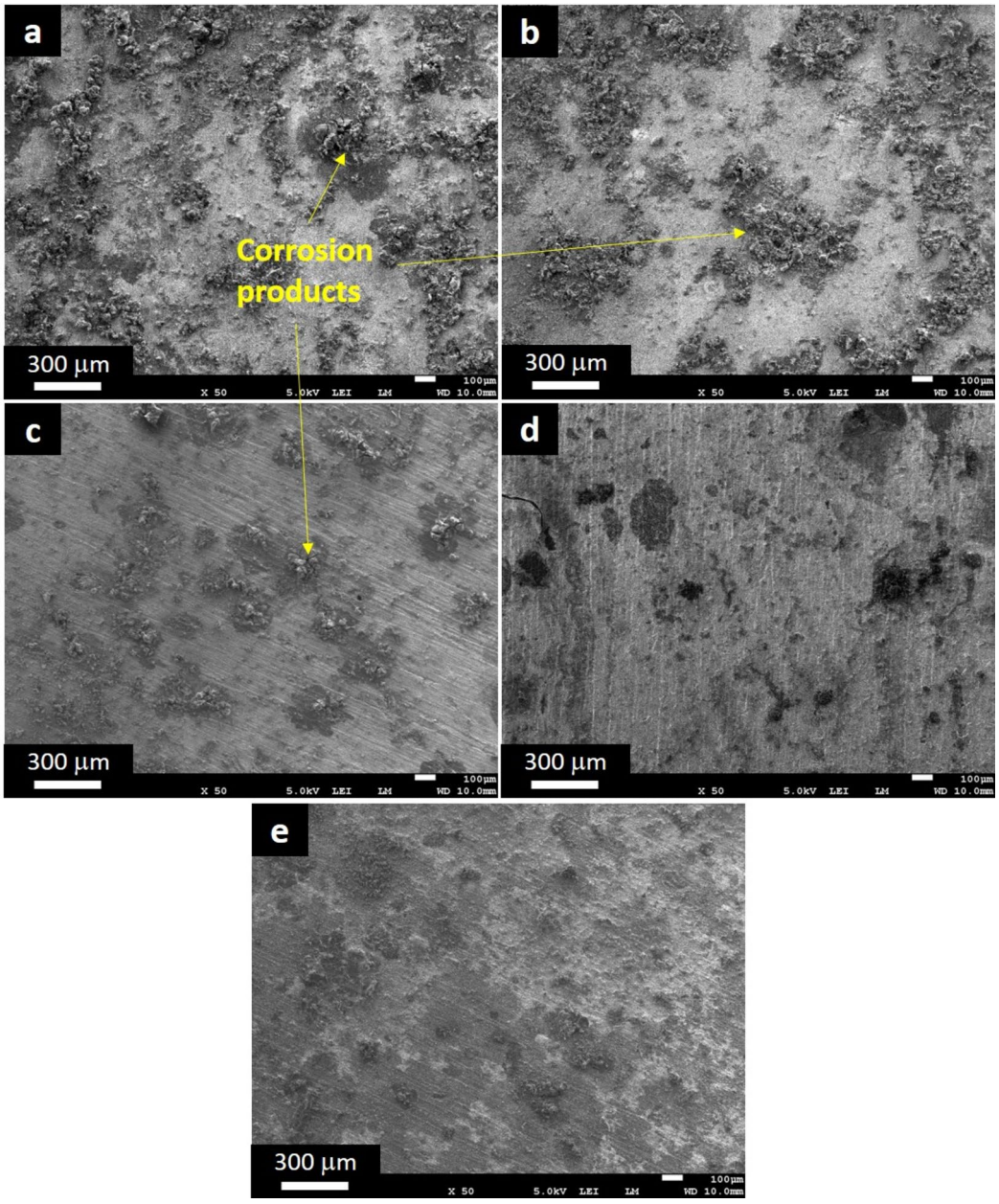

Fig. 10. SEM images of the corrosion surface after 72 h. immersion time for the Al/Biochar composite samples with different volume fraction of the biochar reinforcement, (**a**) Pure Al, AB0, (**b**) AB2.5, (**c**) AB5, (**d**) AB7.5, and (**e**) AB10.

were employed for the investigations. Characterization techniques such as field-emission scanning electron microscopy (FE-SEM).

The electrochemical measurements confirmed the positive effect of biochar addition on the corrosion resistance of the Al matrix. The corrosion resistance was quantitatively described, and it was found that the addition of 10 wt.% biochar resulted in a significant improvement of up to 73.87% after 24 h of immersion in the 3.5% NaCl solution. Mechanical assessments, including compressive strength and hardness, demonstrated a notable enhancement in the mechanical properties of the composites with biochar incorporation. The composite containing 7.5 wt.% biochar exhibited an optimal balance, with an 8.83% increase in compressive strength and a 15.15% rise in hardness compared to the base aluminum matrix. These findings highlight the potential of biochar reinforcement in enhancing the corrosion resistance and mechanical properties of the Al matrix. The optimized composition of 7.5 wt.% biochar showed promising results in achieving a balance between improved mechanical strength and corrosion resistance.

Data availability

The datasets used and/or analysed during the current study available from the corresponding author on reasonable request.

Received: 16 January 2024; Accepted: 22 August 2024
Published online: 27 August 2024

References

1. Cui, Y., Wang, L. & Ren, J. Multi-functional SiC/Al composites for aerospace applications. *Chin. J. Aeronaut.* **21**, 578–584. https://doi.org/10.1016/S1000-9361(08)60177-6 (2008).
2. Sharma, V. K., Kumar, V. & Joshi, R. S. Investigation of rare earth particulate on tribological and mechanical properties of Al-6061 alloy composites for aerospace application. *J. Mater. Res. Technol.* **8**, 3504–3516. https://doi.org/10.1016/J.JMRT.2019.06.025 (2019).
3. Pozdniakov, A. V. *et al.* Development of Al-5Cu/B4C composites with low coefficient of thermal expansion for automotive application. *Mater. Sci. Eng. A* **688**, 1–8. https://doi.org/10.1016/J.MSEA.2017.01.075 (2017).
4. Bhanuprakash, L., Thejasree, P., John, F. & Prabha, R. Study on mechanical and micro-structural properties of aluminium matrix composite reinforced with graphite and granite fillers. *Mater. Today Proc.* https://doi.org/10.1016/J.MATPR.2023.06.243 (2023).
5. Zhu, T. *et al.* A composite pore-structured superhydrophobic aluminum surface for durable anti-icing. *J. Mater. Res. Technol.* https://doi.org/10.1016/J.JMRT.2023.11.250 (2023).
6. Yadav, R. & Ramakrishna, W. Biochar as an environment-friendly alternative for multiple applications. *Sustain.* **15**, 13421. https://doi.org/10.3390/SU151813421 (2023).
7. Rawat, S., Wang, C. T., Lay, C. H., Hotha, S. & Bhaskar, T. Sustainable biochar for advanced electrochemical/energy storage applications. *J. Energy Storage* **63**, 107115. https://doi.org/10.1016/J.EST.2023.107115 (2023).
8. Amalina, F., Krishnan, S., Zularisam, A. W. & Nasrullah, M. Recent advancement and applications of biochar technology as a multifunctional component towards sustainable environment. *Environ. Dev.* **46**, 100819. https://doi.org/10.1016/J.ENVDEV.2023.100819 (2023).
9. Zhu, H. *et al.* Emerging applications of biochar: A review on techno-environmental-economic aspects. *Bioresour. Technol.* **388**, 129745. https://doi.org/10.1016/J.BIORTECH.2023.129745 (2023).
10. Mishra, R. K. & Mohanty, K. A review of the next-generation biochar production from waste biomass for material applications. *Sci. Total Environ.* **904**, 167171. https://doi.org/10.1016/J.SCITOTENV.2023.167171 (2023).
11. Zhang, Q., Cai, H., Yang, K. & Yi, W. Effect of biochar on mechanical and flame retardant properties of wood–plastic composites. *Results Phys.* **7**, 2391–2395. https://doi.org/10.1016/J.RINP.2017.04.025 (2017).
12. Suarez-Riera, D., Falliano, D., Restuccia, L. & Ferro, G. A. The influence of industrial biochar on mortar composites' mechanical properties. *Proc. Struct. Integr.* **47**, 698–704. https://doi.org/10.1016/J.PROSTR.2023.07.050 (2023).
13. Mozrall, A. M., Hernandez-Charpak, Y. D., Trabold, T. A. & Diaz, C. A. Effect of biochar content and particle size on mechanical properties of biochar-bioplastic composites. *Sustain. Chem. Pharm.* **35**, 101223. https://doi.org/10.1016/J.SCP.2023.101223 (2023).
14. Billah, M. M., Jamal, M., Banu, T. & Hasanuzzaman, M. Carbon nanotube reinforced aluminum matrix composite: Recent advances and future prospects. *Ref. Modul. Mater. Sci. Mater. Eng.* https://doi.org/10.1016/B978-0-323-96020-5.00038-8 (2023).
15. Zhang, Y., Wang, W., Liu, J., Wang, T. & Li, T. J. Fabrication of carbon fiber reinforced aluminum matrix composites by inorganic binders. *J. Alloys Compd.* **968**, 172213. https://doi.org/10.1016/J.JALLCOM.2023.172213 (2023).
16. Gu, D. *et al.* Laser additive manufacturing of carbon nanotubes (CNTs) reinforced aluminum matrix nanocomposites: Processing optimization, microstructure evolution and mechanical properties. *Addit. Manuf.* **29**, 100801. https://doi.org/10.1016/J.ADDMA.2019.100801 (2019).
17. Abdo, H. S. *et al.* Ecofriendly biochar as a low-cost solid lubricating filler for LDPE sustainable biocomposites: Thermal, mechanical, and tribological characterization. *Int. J. Polym. Sci.* **2023**, 1–13. https://doi.org/10.1155/2023/2445472 (2023).
18. Zhang, G., Zhu, X., Yu, M. & Yang, F. Electrochemical activation of peroxymonosulfate using chlorella biochar modified flat ceramic membrane cathode for berberine removal: Role of superoxide radical and mechanism insight. *Sep. Purif. Technol.* **318**, 124002. https://doi.org/10.1016/J.SEPPUR.2023.124002 (2023).
19. Udayam Fernandes, P. Novel carbon nanotube and fly-ash reinforced Al composites for automobile and aerospace applications. *Mater. Today Proc.* **35**, 456–460. https://doi.org/10.1016/J.MATPR.2020.02.969 (2021).
20. Jannet, S. *et al.* Effect of neem seed biochar on the mechanical and wear properties of aluminum metal matrix composites fabricated using stir casting. *Mater. Today Proc.* **56**, 1507–1512. https://doi.org/10.1016/J.MATPR.2021.12.572 (2022).
21. ASTM E9-89a(2000) E9 Standard Test Methods of Compression Testing of Metallic Materials at Room Temperature. https://www.astm.org/e0009-89ar00.html (accessed 24 Dec 2023).
22. Xu, G., Lv, Y., Sun, J., Shao, H. & Wei, L. Recent advances in biochar applications in agricultural soils: Benefits and environmental implications. *CLEAN Soil Air Water.* **40**, 1093–1098. https://doi.org/10.1002/CLEN.201100738 (2012).
23. Das, C., Tamrakar, S., Kiziltas, A. & Xie, X. Incorporation of biochar to improve mechanical, thermal and electrical properties of polymer composites. *Polymers.* **13**, 2663. https://doi.org/10.3390/POLYM13162663 (2021).
24. Abdo, H. S., Samad, U. A., Abdo, M. S., Alkhammash, H. I. & Aijaz, M. O. Electrochemical behavior of inductively sintered Al/TiO_2 nanocomposites reinforced by electrospun ceramic nanofibers. *Polymers.* **13**, 4319. https://doi.org/10.3390/POLYM13244319 (2021).
25. Singh, A. K., Shukla, S. K., Singh, M. & Quraishi, M. A. Inhibitive effect of ceftazidime on corrosion of mild steel in hydrochloric acid solution. *Mater. Chem. Phys.* **129**, 68–76. https://doi.org/10.1016/J.MATCHEMPHYS.2011.03.054 (2011).
26. Abdo, H. S., Seikh, A. H., Mohammed, J. A. & Uzzaman, T. Ameliorative corrosion resistance and microstructure characterization of 2205 duplex stainless steel by regulating the parameters of pulsed nd: Yag laser beam welding. *Metals (Basel).* https://doi.org/10.3390/MET11081206 (2021).
27. Abdo, H. S., Samad, U. A., Mohammed, J. A., Ragab, S. A. & Seikh, A. H. Mitigating corrosion effects of Ti-48Al-2Cr-2Nb alloy fabricated via electron beam melting (EBM) technique by regulating the immersion conditions. *Crystals.* **11**, 889. https://doi.org/10.3390/CRYST11080889 (2021).
28. Seikh, A. H., Baig, M., Ammar, H. R. & Alam, M. A. The influence of transition metals addition on the corrosion resistance of nanocrystalline Al alloys produced by mechanical alloying. *Metals.* **6**, 140. https://doi.org/10.3390/MET6060140 (2016).
29. Abdo, H. S., Samad, U. A., Mohammed, J. A., Ragab, S. A. & Seikh, A. H. Mitigating corrosion effects of ti-48al-2cr-2nb alloy fabricated via electron beam melting (Ebm) technique by regulating the immersion conditions. *Crystals* **11**, 889. https://doi.org/10.3390/cryst11080889 (2021).
30. Abdo, H. S. *et al.* Microstructural characterization and corrosion-resistance behavior of dual-phase steels compared to conventional rebar. *Crystals* **10**, 1–14. https://doi.org/10.3390/cryst10111068 (2020).
31. Wang, X. *et al.* Nano-modified functional composite coatings for metallic structures: Part I-Electrochemical and barrier behavior. *Surf. Coat. Technol.* **401**, 126286. https://doi.org/10.1016/j.surfcoat.2020.126286 (2020).

Acknowledgements
The author extends his appreciation to the Researchers Supporting Project number (RSPD2024R597), Kind Saud University, Riyadh, Saudi Arabia.

Author contributions
The author (I.A.) made substantial contributions to the conception, design, acquisition, analysis, and interpretation of the research.

Competing interests
The author declares no competing interests.

Additional information
Correspondence and requests for materials should be addressed to I.A.A.

Reprints and permissions information is available at www.nature.com/reprints.

Publisher's note Springer Nature remains neutral with regard to jurisdictional claims in published maps and institutional affiliations.